Lawrence Berkeley National Laboratory

Title
RADIATION CHEMISTRY OF HIGH ENERGY CARBON, NEON AND ARGON IONS: INTEGRAL YIELDS FROM FERROUS SULFATE SOLUTIONS

Permalink
https://escholarship.org/uc/item/1ng4q2zr

Author
Christman, E.A.

Publication Date
1980-07-01

Lawrence Berkeley Laboratory
UNIVERSITY OF CALIFORNIA
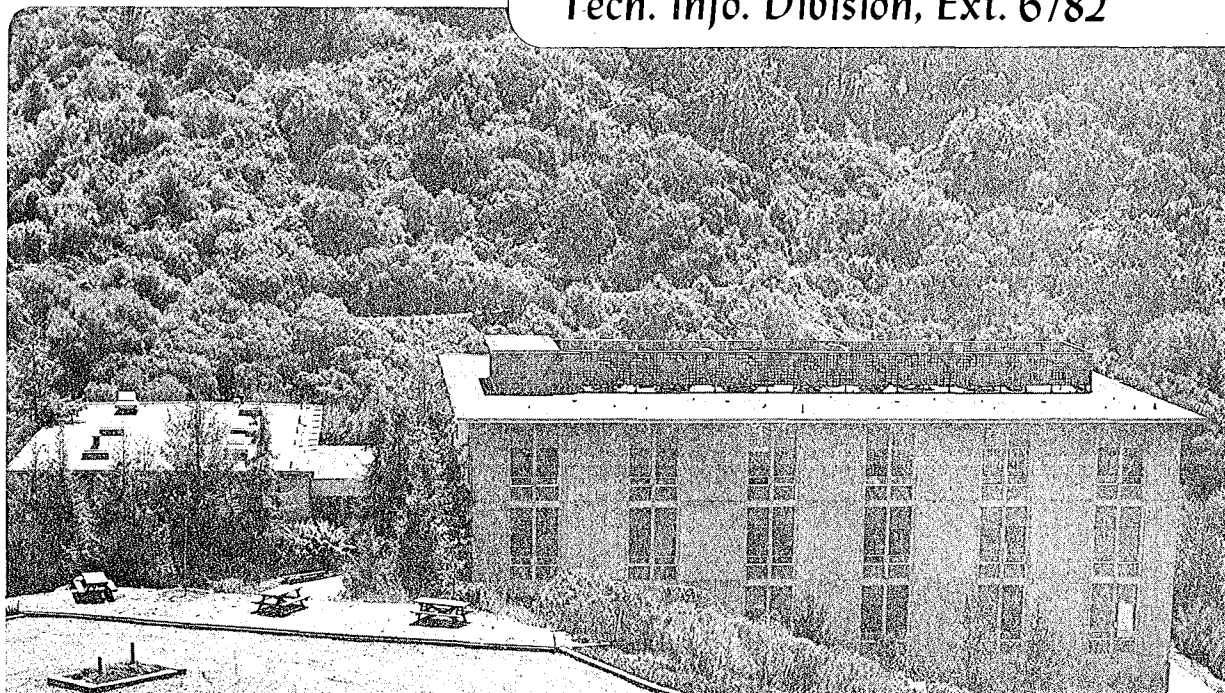
Materials & Molecular Research Division

RADIATION CHEMISTRY OF HIGH ENERGY CARBON, NEON AND ARGON
IONS: INTEGRAL YIELDS FROM FERROUS SULFATE SOLUTIONS

E. A. Christman, A. Appleby, and M. Jayko

July 1980

RADIATION CHEMISTRY OF HIGH ENERGY CARBON, NEON AND ARGON IONS:

INTEGRAL YIELDS FROM FERROUS SULFATE SOLUTIONS

E. A. Christman and A. Appleby

Radiation Science Department
Rutgers State University
New Brunswick, New Jersey 08903

and

M. Jayko

Materials and Molecular Research Division
Lawrence Berkeley Laboratory
University of California
Berkeley, California 94720

ABSTRACT

Chemical yields of Fe^{3+} have been measured from $FeSO_4$ solutions irradiated in the presence and absence of oxygen with carbon, neon, and argon ions from the Berkeley Bevalac facility. $G(Fe^{3+})$ decreases with increasing beam penetration and with increasing atomic number of the incident ion. The results are compared with current theoretical expectations of the behavior of these particles in an aqueous absorber. The chemical yields are consistently higher than theoretically predicted, by amounts varying from <6.2% (carbon ions) to <13.2% (argon ions). The additional yields are possibly attributable to fragmentation of the primary particle beams.

INTRODUCTION

The availability (since 1972) of energetic heavy ions having a range on the order of centimeters in tissue-equivalent material[1,2] has made it possible to study directly for the first time the variations in the radiation chemisty of aqueous solutions as a function of incident particle parameters such as LET and atomic number, Z. Such studies contribute to our knowledge of basic chemical reactions generated by ionizing radiation as well as characterizing the properties of the track structure of these heavy ions in tissue-like material.

We have studied the response of several commonly used radiation chemistry systems to the beams of carbon (Z = 6), neon (Z = 10), and argon (Z = 20) ions generated by the Bevalac at the Lawrence Berkeley Laboratory. We report here on one system, aqueous ferrous sulfate. It is perhaps the best understood system in radiation chemistry. For low LET radiations at least, the mechanism is understood and the availability of experimental data with which to compare our results persuaded us to emphasize it.

According to radiation chemistry theory the passage of an ionizing particle through an aqueous solution generates hydrated electrons, H atoms, H_3O^+ and OH in discrete regions termed spurs.[3] H_2 and H_2O_2 are formed within the spurs and all of these entities diffuse from the point of origin. The "yields" of these entities remaining at long times (10^{-7} seconds) are affected by the LET and charge of the particle and by the presence of solutes capable of reacting with them ("scavengers").

For low LET radiation (high energy electrons) the chemical reactions take place within individual spurs which are essentially isolated from each other. As the LET increases however, the distance between spurs decreases so that, increasingly, the radicals from adjacent spurs react

with each other to form the molecular products, increasing the molecular product yields. If a scavenger is present this increased molecular product yield is at the expense of the radical-scavenger reactions.

It has been assumed that the yields of e^-_{aq}, H, OH, and H_3O^+ at the very earliest times are independent of LET and that excited electronic states are not important. The measured yields of both the molecular and radical products however are dependent on the LET but not uniquely so. For example, previous studies[4,5,6] have shown that for particles of the same mean LET, $G(Fe^{+3})$ from irradiated ferrous sulfate solutions decreases as the atomic number, Z, of the particle increases. ('G' expresses the yield in molecules per 100 eV).

The earlier studies suffered from an unavoidable problem. The kinetic energy of the particles was low enough that the particle range was on the order of a few millimeters at best. Because the LET is proportional to the reciprocal of the square of the speed of the particles it varied rapidly and considerable over the short range of the particles so that system measurements at a constant LET value were impossible. Thus only a weighted mean value for an average LET was obtained. The more energetic particles we have used in this work have a "plateau" region in which the LET remains relatively constant for a distance of several centimeters (see Fig. 1). Thus a beam of particles passing through a system at this point has a nearly constant value for the LET. So for the first time we are able to measure the response of the chemical systems to a nearly constant, single valued LET.

EXPERIMENTAL

The irradiated systems were 10^{-2} M Ferrous Sulfate in 0.4 M sulfuric acid with 10^{-3} M sodium chloride (to inhibit interferences from organic impurities). All chemicals were reagent grade and made up in triple distilled water (distilled water redistilled from alkaline permanganate and then from phosphoric acid).

In the oxygen-free systems, nitrogen was bubbled through the systems for a minimum of 20 minutes immediately before the irradiation.

The irradiations were done in quartz cells, 3.2 cm in diameter with a particle path length of 1.0 cm. The cell window thicknesses ranged from 1.65 - 1.80 mm and were parallel to ±0.025 mm. They were fitted with necks 10 - 12 cm long with ground glass stoppers. The cell volumes were 8.3 ml, providing enough irradiated solution for optical measurement after a relatively short irradiation time. All glassware was rinsed with triple distilled water and baked at 1140°C for eight hours to remove any organic impurities.

The cells were used in sets of eight matched according to window thickness so that several sets could be used interchangeably. The cells were placed along the beam such that the entire range of the heavy ions was covered (Figure 1), and in a typical run the variable water column was adjusted to place the Bragg peak in the sixth cell downstream one to two millimeters from the inner face of its rear window. The peak was positioned to within 0.5 mm. Several runs were conducted with no water column absorption by adding enough cells to place the full energy beam Bragg peak in the third cell from the rear of the stack. As many as 16 cells were used in these runs.

The beam diameter was adjusted by the machine focusing magnets to give a one sigma diameter of about one centimeter which placed about 99 percent of the beam within the irradiated cell volume. The beam size, cross sectional shape and position with respect to the cells was monitored by exposing Polaroid film behind a single cell.

The beam particle incident kinetic energy was determined from machine parameters. The maximum energies entering the target solutions were: carbon 375 MeV/amu; neon 520 MeV/amu; argon 445 MeV/amu. The relative ionization along the Bragg curve, the absorbed dose rate and the accumulated absorbed dose were measured by the ion chambers[7] mounted on the beam line. The absorbed dose rates were in the range of 20 to 30 Grays per minute as measured on the 3.0 cm ring of the ion chamber immediately upstream of the target. The total entrance dose ranged from 20 to 150 Grays. The measurements are believed to be accurate to five percent (1σ), and have been made assuming $\overline{W}$ = 36.4 ± 0.06, 35.4 ± 0.8 and 34.7 ± 0.5 ev/i.p. for carbon, neon and argon ions respectively[8] in nitrogen, and that the mass stopping power in water relative to nitrogen is 1.125.[7]

Ferric yields were measured within five minutes of the end of the irradiation using a Beckman DU spectrophotometer. The optical density was measured at 304 nm in one centimeter cells. The extinction co-efficient was taken as 2170 ± 20 M^{-1} $1.cm^{-1}$ at 25°C. Temperature corrections were made as necessary.

A Bragg curve of $-dE/dx$ versus x was measured during each experimental run. Integration of this curve between the limits of x corresponding to the position of each glass cell gave a dose correction (D.C.) value for that particular position. The dose in each cell was obtained by multiplying the D.C. value by the dose obtained from the ion chamber immediately upstream

of the stack of cells. An approximately eight percent correction was made to the 3.0 cm ion chamber readings for the 3.2 cm cell diameter. G-values were obtained as a function of Q, the distance from the Bragg Peak, for a given ion by means of a general linear regression model in which Q appears as a classification variable, using the Statistical Analysis System installed on the Rutgers IBM 360/370 computer, employing all the data available for that particular ion. The curves shown in Figs. 2, 3, and 4 result respectively from 122, 197 and 77 data points for aerated ferrous solutions, and 40, 168 and 78 data points for deaerated ferrous solutions. Only data obtained from cells upstream of the Bragg Peak have been utilized in the present analysis.
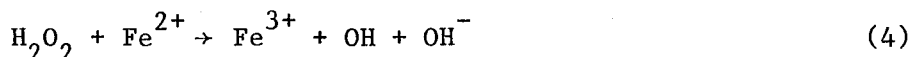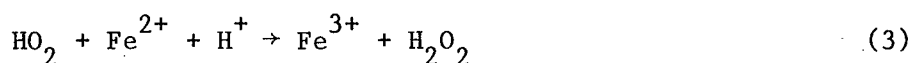
RESULTS

The measured $G^i(Fe^{3+})$ values as a function of distance upstream of the Bragg Peak, or residual range, for carbon, neon and argon ions are shown respectively in Figs. 2, 3 and 4 for both aerated and deaerated ferrous sulfate solutions. The dotted lines indicate one standard deviation for random errors (inner pair) and for combined random and systematic errors (outer pair). The sources of these errors will be discussed later. In all cases there is a substantial fall-off in G-value as the Bragg peak position is approached. There is also a significant decrease in G-value for a given residual range as the charge on the incident ion increases.

Figure 5 shows the data for all three ions plotted as a function of z^2/β^2 where Z is the charge on the ion and β is its velocity relative to that of light. This parameter has been proposed[9] to replace stopping power when the radius of the sensitive volume is much less than the range of delta rays. This criterion is amply fulfilled for these very energetic ions. Figure 6 is a comparison of our data for aerated $FeSO_4$ solutions with data from the literature.

In Figure 8 we present a comparison of our present results for aerated ferrous sulfate with the predictions of a theoretical model.[10]

DISCUSSION

The results shown in Figs. 2, 3 and 4 are qualitatively in agreement with current models of the radiation chemistry of aqueous systems as they pertain to heavy charged particles.[3] The yields of the observed product, Fe^{3+} are due principally to reactions 1 - 4

$$OH + Fe^{2+} \rightarrow Fe^{3+} + OH^-$$ (1)

$$H + O_2 \rightarrow HO_2$$ (2)

$$HO_2 + Fe^{2+} + H^+ \rightarrow Fe^{3+} + H_2O_2$$ (3)

$$H_2O_2 + Fe^{2+} \rightarrow Fe^{3+} + OH + OH^-$$ (4)

occuring in systems containing dissolved air, with reaction 2a

$$H + H^+ + Fe^{2+} \rightarrow H_2 + Fe^{3+}$$ (2a)
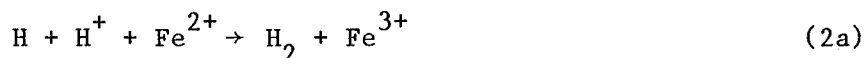
in place of 2 and 3 when oxygen is absent.

For any given particle of charge Z and Energy E the product yield $G^i(Fe^{3+})$ is therefore determined by the yields $G^i(Z,E)$ of the reactive intermediates H, OH, and H_2O_2, according to

$$G^i(Fe^{3+})_{air} = 3G_H^i + G_{OH}^i + 2G_{H_2O_2}^i$$ (5)

$$G^i(Fe^{3+})_{N_2} = G_H^i + G_{OH}^i + 2G_{H_2O_2}^i$$ (6)

where the suffixes indicate yield measured in solutions equilibrated respectively with air and nitrogen. (The term G_H^i is taken to include the yield of both H and e_{aq}^-, since these experiments were all done in the presence

of a high H_3O^+ concentration, where $e_{aq}^- + H_3O^+ \rightarrow H + H_2O$ occurs very rapidly.)

It is well established[3] that for particles of short range, where all the energy is lost in the irradiated solution, the observed or "integral" Ferric yields for a particle of initial energy E, as given for example by

$$G^o(Fe^{3+})_{air} = 3G_H^o = G_{OH}^o + 2G_{H_2O_2}^o$$

$$= \frac{1}{E} \int_E^o G^i(Fe^{3+})_{air} \, dE = \frac{1}{E} \int_E^o (3G_H^i + G_{OH}^i + 2G_{H_2O_2}^i) \, dE$$

decrease with decreasing E as a net result of the changing yields of reactive intermediates as the particle slows down.

The separate variation of "integral" yields G^o with E of the important reactive species has been deduced from experiments using a variety of chemical systems and it is clear that the overall behavior of the ferric yield is dominated by the pronounced decreases in G_H^o and G_{OH}^o with decreasing E.

In the present study we have measured "instantaneous" or differential track-segment G-values, with a resolution equivalent to the cell thickness, 1 cm. In most previous work with charged particles, energies were much lower and the ions were usually completely stopped within the test solution. The G-values so obtained were therefore "integral" for all energies below the entrance value.

The earliest, and still the most extensive measurements on effects of energetic positive ions on the $FeSO_4$ system were by Schuler and Allen[4] and Hart, Ramler and Rochlin.[5] They respectively measured "instant" $G^i(Fe^{3+})$ values from essentially the slope of plots of $G^o \times E^o$ versus E^o, where E^o

is the entrance energy and G^o the average yield over the entire range of the ion.

Collinson, Dainton and Kroh[11] measured ferric yields from solutions irradiated with ^{210}Po α-particles. They used thin absorbers to allow different fractions of the α-particle tracks to be spent within the solution. $G^i(Fe^{3+})$ values were calculated for track elements throughout the range of penetration of the ions.

Schimmerling et al.[12] reported $G(Fe^{3+}) = 11.3 \pm 0.9$ for the "plateau" region (180-420 MeV cm^2/g of high energy nitrogen ions). As the stopping power increases less than two-fold in this region the chemical yield can be taken to be approximately the average differential yield over the 8.5 $g.cm^{-2}$ of the Bragg curve "plateau".

More recently[13] the "instantaneous" or "differential" yield of the hydrated electron has been measured by pulse radiolysis for deuterons and α particles of initial energies 20 and 40 MeV respectively, and shows the expected decrease as the particles slow down.

It is therefore entirely to be expected that the integral Fe^{3+} yields measured in the present work decrease with particle penetration, as is observed (Figs. 2, 3 and 4).

Traditionally, radiation chemical yields for particles of different charge and energy have been reported in terms of some kind of LET- most frequently the stopping power, dE/dx, or LET_∞. Diffusion kinetic calculations have used the same quantity. dE/dx has the advantage of, in effect, combining particle charge and velocity (or energy) into a single parameter. Unfortunately particles having the same dE/dx but different velocities or charges do not have common G^o values for the reactive intermediates nor, as a result, for measured product yields. The discontinuities that have

been reported in plots of G versus dE/dx for various ions[4,5,13,14] are the result of changes in the structure of tracks with ion velocity and charge, which have been predicted on theoretical grounds.[15,16,17] At increased velocity of a given ion, the proportion of energy deposited in a diffuse geometry (the "penumbra" in the terminology of Magee and Chatterjee[10] increases at the expense of the denser track "core", encouraging radical escape and increasing the fraction of radicals available for reaction with solutes at long times ($>10^{-7}$ sec).

For two ions of the same stopping power, the faster, and necessarily more highly charged ion will thus produce a geometry less conducive to radical recombination, with higher G (radical) values and, in the ferrous systems, larger $G(Fe^{3+})$. These effects have been discussed recently by Sauer et al.[13] who, following suggestions of Katz[9] have used the parameter Z^2/β^2 instead of dE/dx in analyzing their data for $^2H^+$ and $^4He^{2+}$. G-values plotted against Z^2/β^2 showed considerably less discontinuity between the results for these two ions than did plots using dE/dx. They concluded that this quantity more effectively describes the rates of intratrack reactions on which the observed yields of radicals and products depends, than does dE/dx.

Figure 5 shows our data for Fe^{3+} G-values plotted as a function of Z^2/β^2. The random error (1σ) is indicated. Within the limits of error no significant discontinuity exists between plots for the three ions, providing further support for the greater usefulness of this quantity.

Figure 6 shows our aerated $FeSO_4$ data with data from Refs. 4, 5, 12 and 14, plotted against Z^2/β^2. The data from Ref. 11 is not included as this was for low energy alphas near the end of their range where charge exchange renders the effective value of Z uncertain. The data from Ref. 5

has been normalized upward by 3% to eliminate discrepancies caused by use of different charge displacement factors (in the cell windows used) and different ferric ion extinction coefficients by those workers as compared with Schuler and Allen.[4] The present data aligns with the literature values for Z^2/β^2 up to about 300, within experimental errors, but above this appears to show generally higher G-values than the extensive data from accelerated protons and α particles.[4,5]

That some additional source of radical intermediate is present in high energy heavy ion radiolysis is also indicated by a comparison of our data with that of Sauer et al.[18] We can obtain an estimate of the sum $G_e^i + G_H^i$ by manipulating our data for aerated and deaerated $FeSO_4$ solutions. It is easy to show that

$$1/2 \ (G^i(Fe^{3+})_{air} - G^i(Fe^{3+})_{N_2}) = G_e^i + G_H^i \quad .$$

This quantity is shown in Fig. 7 for carbon ion radiolysis as a function of Z^2/β^2. Sauer et al.[18] measured ferric yields as a function of time following pulse radiolysis with $^2H^+$ (16-20 MeV) and $^4He^{2+}$ (24-40 MeV). They were able to calculate radical and molecular yields from their data and their values of $G_e^i + G_H^i$ are also shown in Fig. 7. The difference between the light and heavy ion data corresponds to a G-value of about 0.4 ± 0.3, implying apparently an additional yield of this many hydrated electrons per 100 eV in our experiments, since we expect G_H^i to be fairly independent of ionization density.[19]

We can also estimate roughly the increase in G_e^i on going from light to heavy ions of the same Z^2/β^2 by comparing the ferric yields obtained previously[4,5] in steady state radiolysis of aerated ferrous sulfate with the present data. An increase in G_e^i in this system would lead to a

3-fold increase in $G^i(Fe^{3+})$ because of the stoichiometry of the overall

oxidation (Eq. 5). A further increase would be expected from a concomitant

increase in G^i_{OH}, which is roughly equal to G^i_e. We therefore expect

that an increase of G^i_e would produce an additional yield of Fe^{3+} of

about $4\Delta G^i_e$. (This is an upper limit since it neglects a probable slight

decrease in $G^i_{H_2O_2}$).

From the actual differences between our data and the previous work

with light ions[4,5] we find G^i_e varies from about 0.05 ± 0.15 (random error)

at $z^2/\beta^2 = 100$ to about 0.5 ± 0.14 at $z^2/\beta^2 = 700$. This is in reasonable

agreement with the ΔG^i_e values derived from a consideration of the recent

pulse radiolysis data,[7] considering the nature of the comparison.

Diffusion kinetics has been the most prominent and useful mathematical

tool for studying the chemical behavior of irradiated liquid systems,

especially dilute aqueous solutions.[20,21] Chatterjee and Magee[10] have

recently applied this approach specifically to high energy heavy ions and

in particular have calculated differential Fe^{3+} yields for irradiated $FeSO_4$

solutions and compared them with published experimental data including

preliminary results of the work reported here.[22] Some results of their

calculations, together with the present data, are shown in Fig. 8.

It is clear that, while the general trend of the data parallels quite

nicely the results from the model, the experimental values are consistently

higher than predicted. Further, the magnitude of the discrepancy is similar

to the differences between our data and the previous work with light ions.

Possible reasons for these discrepancies will now be discussed.

1. Random Experimental Errors

The standard deviations for the three ions, in terms of G-values, calculated from yield/dose plots as described above are: carbon ±0.39, neon ±0.47, argon ±0.43. These are given in Table I as percentage of G-value for ions of various energies.

While in the case of carbon these deviations are within about 2σ of the model predictions,[10] some of the neon and argon data are outside these limits.

Further, all the deviations are in the same direction of underestimating the experimental values. Clearly some explanation other than random error is required, especially for neon and argon.

2. Dosimetry Errors

As discussed above, dosimetry was based on

(a) ion chamber calibration traceable to ^{14}C activation for the incident beam flux;

(b) Bragg curve measurements done prior to each experimental run.

The possibility of a systematic error in (a) exists. It is believed to be < 5%.[8]

Such an error would probably be in the same direction for all ions, and could partially explain the non-random pattern of deviation directions in Table I. The effect of including the maximum 5% systematic error is also shown in Figs. 2, 3 and 4.

We also believe errors exist in the Bragg curve procedure (b above). Slight but distinct differences in the shape of the Bragg Peaks taken prior to different experimental runs were noted. The particular Bragg curve obtained prior to a given run was used for dose integration in each cell for that run. This did not affect the dosimetry in the first cell, but

Table I. Analysis of errors, with comparison to Diffusion Kinetic Model.

$FeSO_4$/air data

Ion,	E/amu	G(exp)	G(Model)	Difference %	Random	I.C. Cal	Bragg.	Total
C ,	60	10.14	9.51	− 6.2	3.9	5	2.7	6.9
C ,	100	10.93	10.46	− 4.3	3.6	5	1.4	6.3
C ,	200	12.03	11.6	− 3.6	3.3	5	0.1	6.0
C ,	300	12.53	12.14	− 3.1	3.1	5	0.2	5.9
Ne ,	80	9.28	8.24	−11.2	5.1	5	3.3	7.9
Ne ,	100	9.68	8.58	−11.4	4.9	5	2.4	7.4
Ne ,	200	10.82	9.62	−11.1	4.4	5	0.2	6.7
Ne ,	300	11.12	10.18	− 8.5	4.3	5	0.7	6.6
Ar ,	100	8.05	7.19	−10.7	5.4	5	3.1	8.0
Ar ,	200	9.00	7.92	−12.0	5.3	5	2.3	7.6
Ar ,	300	9.60	8.33	−13.2	5.0	5	2.2	7.4

differences in the Bragg curve used would have resulted in progressively greater differences at greater penetration depths. To assess the magnitude of such an effect we have recalculated our data using a single "average" Bragg curve for dose integration. As an example, a comparison of results obtained by these two procedures for the worst case, carbon, is shown in Fig. 5. where the dashed line is calculated using the "average" Bragg curve. In general, differences between the two methods of calculation are quite small until positions within about 4 cm of the Bragg Peak. Differences then become greater, until at 1 cm from the peak they amount to about 3%. It is interesting to note that the degree of scatter on the data is entirely unchanged with carbon, and somewhat improved with neon and argon by the use of "averaged" values for the Bragg curve. We conclude that the differences observed in the two calculation procedures correspond roughly with the error associated with the variations in the experimental Bragg curves used.

Combining all the above sources of error we can make a more meaningful comparison with Chatterjee and Magee's model. Table I shows the model calculation values and the total error limits for the three ions. In all cases the disagreement between the model and the experimental values is within two standard deviations of the combined error. We conclude that the disagreement between the theoretical approach and our data is probably some-what greater than the combined experimental errors, at least for neon and argon. The most obvious cause of this disagreement is beam fragmentation, which is not considered in the present theoretical models. This will therefore be discussed next.

3. Effects Due to Fragmentation of the Primary Beam

It is certain that in the case of all three ions, inelastic collisions with atoms in the experimental arrangement (silicon and oxygen in the glass cell windows, oxygen and hydrogen in the water column and solutions) will result in some degree of fragmentation of the main beam,[23] so that the energy deposited at depth is due to less massive particles, as well as to the incident ions. At present the precise extent of these effects is unknown, and though some cross-section data have been published[23] they remain insufficient to apply in a truly quantitative manner to our results.

We can, however, consider in a general way how this phenomenon would affect them. Our dosimetry is based upon Bragg curves measured by an ionization chamber. An error ensues due to fragmentation in the upstream water column if the W- values for the primary beam and the small fragment ions are not the same. There is some evidence that this might indeed be the case. Recent measurements of W- values from carbon, nitrogen and argon ion irradiation of nitrogen gas suggest a trend of decreasing W with increasing ion charge.[8] If this trend is real and extends to the lightest fragments, contamination of the beam in our experiments with fragments produced upstream of the ionization chamber (e.g., in the variable water column, Fig. 1) would result in our underestimating dose and thus over-estimating G- values. The magnitude of this effect would depend on the extent of beam fragmentation at the ion chamber used, and on the effective W- value for the fragmented beam. Neither of these quantities is known but based on the available data[8] we estimate the effect on our dosimetry to be certainly less than 1% in the worst case (carbon runs with a long water column).

We now consider the effects of fragmentation on the observed chemistry.
First we note that the interaction cross section increases as the 2/3 power
of the atomic mass of the incident ion[24] so that effects of fragmentation
will be expected to be greater for neon and argon than for carbon in our
experiments. Next, we can observe that fragments will necessarily be of
lower atomic number than the main (or incident) beam. Their velocities
will however be substantially the same as that of the incident heavy ion.
Most fragmentation will result in the removal of only a few nucleons from
the heavy ion, and the larger fragment will differ little from the original
ion in its subsequent chemical effects. The smaller fragments (proton,
neutrons, deuterons and alphas) will produce, per increment of deposited
energy, more free radical chemistry than the parent heavy ion. We there-
fore expect fragmentation to increase the overall chemical yield in our
systems. This increase will not necessarily be uniform with penetration
depth. The small fragments will have a longer range than the large ones
and will deposit energy further downstream.

Another aspect of fragmentation is the number of fragments produced
per collision. If, for example, two deuterons are produced in a given
collision instead of one alpha particle they would probably have about
the same velocity as the alpha, but would produce more free radical
reactions in solution since, as we have seen, chemistry is related roughly
inversely to the square of the particles' charge. The probability of
this type of fragmentation occurring would presumably be related to the
probability of deep (as contrasted to glancing) collisions and on purely
geometrical grounds might be expected to increase with the atomic number
of the incident ion. Such an effect would contribute to greater-than-
expected ferric yields, especially for neon and argon.

Finally, we would expect the spectrum of fragment sizes to shift towards heavier fragments (and away from light ones) as the atomic number of the projectile increases. Chatterjee et al.[23] have calculated from cosmic ray data the fragmentation probabilities in water for incident nitrogen and oxygen nuclei. It is clear that heavier fragments are more important with the heavier (oxygen) ion. If this is a general trend, this effect would tend to decrease the ferric yields for neon and especially argon, since heavier fragments would, in our systems, give less chemistry.

We actually observe the greatest discrepancy between the Chatterjee/ Magee model and our data in the case of intermediate ion, neon. All but the last discussed fragmentation effect (spectrum of fragment sizes) would tend to increase the observed chemical yields and predominately so for the heavier ions. The question therefore arises as to why agreement improves on going from neon to argon. Possibly in the case of argon we have accidental cancelling of this increase by a fragmentation spectrum shifted towards heavy fragments. We must await experimental fragmentation data before these speculations can be thoroughly tested.

Though experimental production cross-sections for fragments are sparse, approximate calculations can be made using an empirical formula derived from the optical or "good geometry" model of fragmentation.[24] The formula is

$$\sigma_{total} = \Pi r_o^2 \left[A_{inc}^{1/3} + A_{tar}^{1/3} - b_o (A_{inc}^{-1/3} + A_{tar}^{-1/3}) \right]^2 .$$

where r_o is a proportionality constant for the geometrical nuclear

radius. It is taken as 1.36;

b_o is an overlap parameter, taken as 0.75;

A_{inc}, A_{tar} are the atomic numbers of the incident and target nuclei.

The fragment production frequencies of O and N on H_2O have been estimated from cosmic ray studies.[23] Taking these values and the total cross-section calculated from the above formula we can make a rough estimate of the number and distribution of fragments in our carbon and neon experiments. (Extrapolation to argon would not seem justified). Then using the predicted $G(Fe^{3+})$ values for each fragment we can obtain a weighted sum for the expected $G(Fe^{3+})$ in our carbon and neon experiments which take fragmentation into account. The results of such a calculation are shown in Fig. 8. It seems possible that fragmentation could indeed account for the higher chemical yields observed, at least in the cases of carbon and neon.

CONCLUSION

The ferric yields from ferrous sulfate solutions irradiated with high energy heavy ions vary with ion charge and beam penetration in a manner consistent with current ideas of heavy ion track structure. The parameter z^2/β^2 is unifying. Fragmentation of the primary beam, resulting in contamination with less densely ionizing particles, could account for the observed ferric yields being higher than predicted theoretically.

ACKNOWLEDGMENTS

REFERENCES

1. M. G. White, M. Isaila, K. Prelec and H. L. Allen, Acceleration of Nitrogen Ions to 7.4 GeV in the Princeton Particle Accelerator, Science, 174, 1121-1123 (1971).

2. H. A. Grunder, W. D. Hartsough and E. J. Lofgren, Acceleration of Heavy Ions at the Bevatron, Science, 174, 1128-1129 (1971).

3. See, e.g., I. G. Draganic and Z. D. Draganic, The Radiation Chemistry of Water, Academic Press, New York (1971).

4. R. H. Schuler and A. O. Allen, Radiation Chemistry Studies with Cyclotron Beams of Variable Energy: Yields in Aerated Ferrous Sulfate Solution, J. American Chemical Society, 79 1565-1572 (1957).

5. E. J. Hart, W. J. Ramler and S. R. Rochlin, Chemical Yields of Ionizing Particles in Aqueous Solution: Effect of Energy of Protons and Deuterons, Radiation Research 4, 378-393 (1956).

6. M. Imamura, M. Matsui, and T. Karasawa, Radiation Chemical Studies with Cyclotron Beams. II. The Radiolysis of an Aqueous Ferrous Ammonium Sulfate Solution with Carbon and Nitrogen Ions, Bulletin of the Chemical Society of Japan, 43, 2745-2749 (1970).

7. J. T. Lyman and J. Howard, Biomedical Research Facilities and Dosimetry In Biological and Medical Research with Accelerated Heavy Ions at the Bevalac 1974-1977. LBL-5610 (1977).

8. R. H. Thomas, J. T. Lyman and T. M. de Castro, A Measurement of the Average Energy Required to Create an Ion Pair in Nitrogen by High-Energy Ions. Radiation Research 82, I-12 (1980).

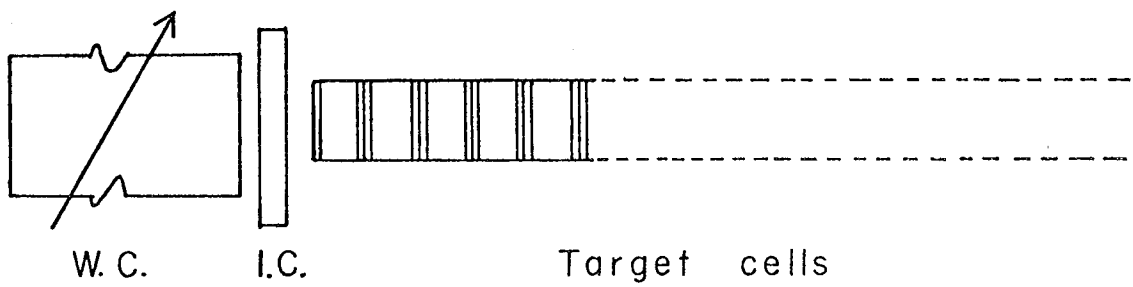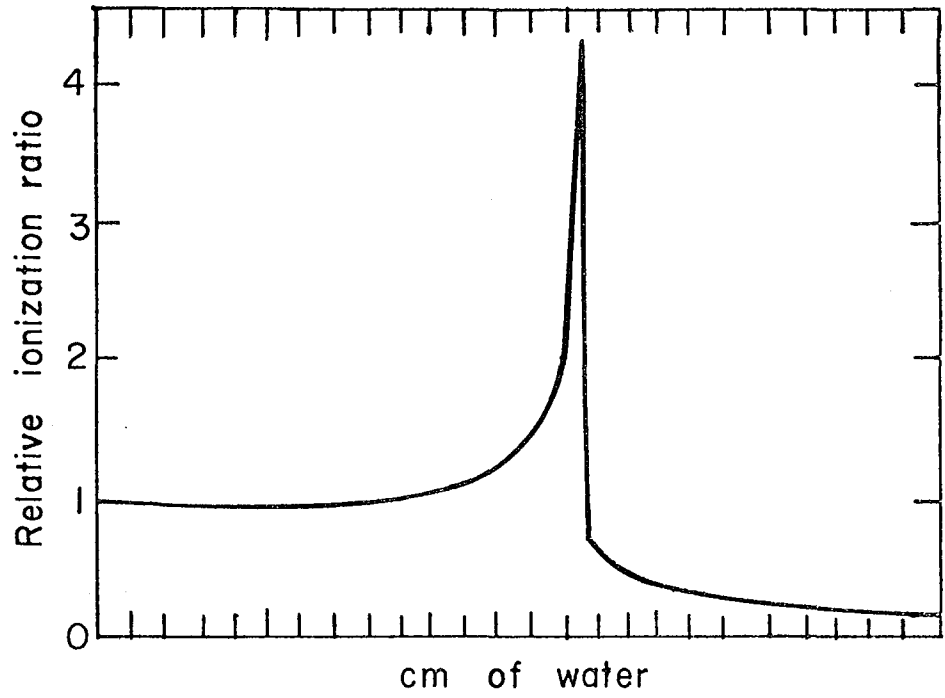9. R. Katz, RBE, LET and Z/β^{α}. Health Physics 18, 175 (1970).

10. A. Chatterjee and J. L. Magee, Relationship of the Track Structure of Heavy Particles to the Physical Distribution and Chemical Effects of Radicals. In Proceedings of the Sixth Symposium on Microdosimetry, Brussels, Belgium, May 22-26, 1978. (J. Booz and H. G. Ebert, Eds) pp. 283-294, Harwood Academic Publishers, London, 1978.

11. E. Collinson, F. S. Dainton and J. Kroh, The Radiation Chemistry of Aqueous Solutions. I. The Effect of Changing Linear Theory Transfer Along a Polonium Alpha-Particle Track. Proc. Royal Soc. 265A, 407-421 (1962).

12. W. Schimmerling, K. G. Vosburgh, P. W. Todd and A. Appleby, Apparatus and Dosimetry for High Energy Heavy-Ion Beam Irradiations. Radiation Research 65, 389-413 (1976).

13. M. C. Sauer, K. H. Schmidt, E. J. Hart, C. A. Naleway and C. D. Jonah, LET Dependence of Transient Yields in the Pulse Radiolysis of Aqueous Systems with Deuterons and Alpha Particles. Radiation Research, 70, 91-106 (1977).

14. A. Appleby and E. A. Christman, Radiation Chemical Studies with 3.9 GeV N^{7+} Ions. Radiation Research, 60, 34-41 (1974).

15. A. Chatterjee, H. D. Maccabee and C. A. Tobias, Radial Cut-off LET and Radial Cut-Off Dose Calculations for Heavy Charged Particles in Water. Radiation Research 54, 479-494 (1973).

16. A. Mozumder, Track-Core Radius of Charged Particles at Relativistic Speed in Condensed Media. Journal of Chemical Physics 60, 1145-1148 (1974).

17. R. H. Ritchie and W. Brandt. Primary Processes and Track Effects in Irradiated Media. In Radiation Research-Biomedical, Chemical and Physical Perspectives. (O.F. Nygaard, H. I. Adler and W. K. Sinclair, Eds.), pp. 315-324. Academic Press, New York, 1975.

18. M. C. Sauer, E. J. Hart, C. A. Naleway, C. D. Jonah and K. H. Schmidt, Pulse Radiolysis with $^2H^+$ and $^4He^{2+}$. Fast and Slow Formation of Fe^{3+} in Acidic Fe^{2+} Solutions. Journal of Physical Chemistry $\underline{82}$, 2246-2248 (1978).

19. A. Appleby and H. A. Schwarz, Radical and Molecular Yields in Water Irradiated by Gamma Rays and Heavy Ions. Journal of Physical Chemistry $\underline{73}$, 1937-1941 (1969).

20. A. Kupperman, Diffusion Kinetics in Radiation Chemistry. In The Chemical and Biological Action of Radiations V (M. Haissinsky, Ed.) pp. 87-166. Academic Press, New York (1961).

21. H. A. Schwarz, Applications of the Spur Diffusion Model to the Radiation Chemistry of Aqueous Solutions. Journal of Physical Chemistry $\underline{73}$, 1928-1937 (1969).

22. M. Jayko, A. Appleby, E. A. Christman, A. Chatterjee and J. L. Magee, Radiation Chemistry of Particles Accelerated at the Bevalac. Lawrence Berkeley Laboratory Report LBL-7432, T.I.D.-4500 - R66 (1978).

23. A. Chatterjee, C. A. Tobias and J. T. Lyman, Nuclear Fragmentation in Therapeutic and Diagnostic Studies with Heavy Ions. In Spallation Nuclear Reactions and their Applications. (Shen and Merker, Eds.), pp. 169-191. D. Reider Publishing Co. Dordrecht, Holland, 1976.

24. H. H. Heckman, D. E. Greiner, P. J. Lindstrom and H. Shwe, Fragmentation of ^4He, ^{12}C, ^{14}N, and ^{16}O Nuclei in Nuclear Emulsion at 2.1 GeV/Nucleon, Lawrence Berkeley Laboratory Report, LBL-3656, (1977).
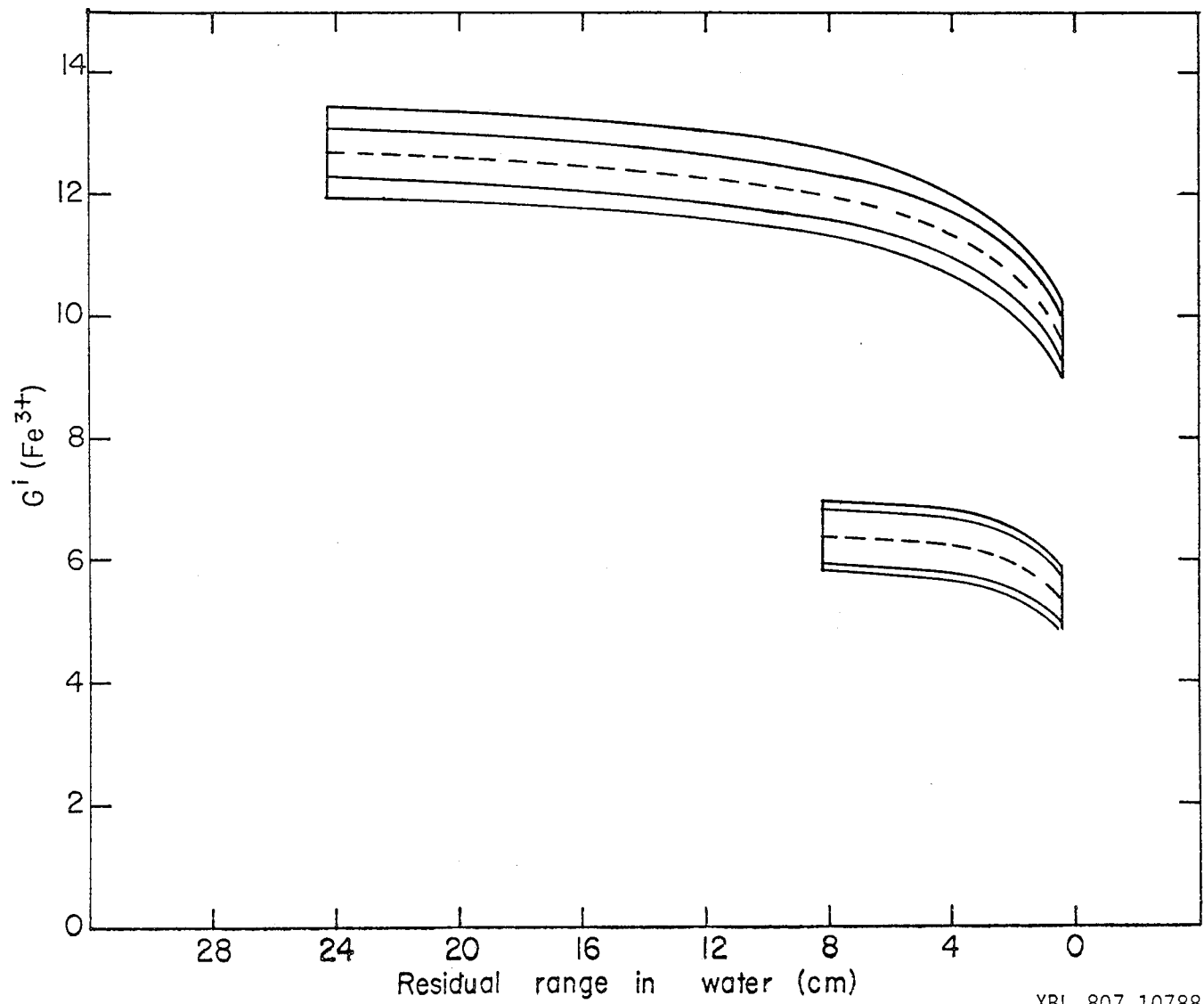
FIGURE CAPTIONS

Fig. 1.   Experimental set-up and typical Bragg curve (carbon); W.C. - Variable water column; I.C. - ionization chamber.

Fig. 2. $G^i(Fe^{3+})$ from aerated (upper curves) and deaerated (lower curves) ferrous sulfate solutions irradiated with carbon ions. Solid lines are error limits - inner pair is 1σ random error; outer pair is 1σ random plus 5% systematic error.

Fig. 3. $G^i(Fe^{3+})$ from aerated (upper curves) and deaerated (lower curves) ferrous sulfate solutions irradiated with neon ions. Solid lines are error limits - inner pair is 1σ random error; outer pair is 1σ random plus 5% systematic error.

Fig. 4. $G^i(Fe^{3+})$ from aerated (upper curves) and deaerated (lower curves) ferrous sulfate solutions irradiated with argon ions. Solid lines are error limits - inner pair is 1σ random error; outer pair is 1σ random plus 5% systematic error.

Fig. 5. $G^i(Fe^{3+})$ from aerated (upper curves) and deaerated (lower curves) ferrous sulfate solutions irradiated with carbon, neon and argon ions, as a function of Z^2/β^2. 1σ random error indicated. Dashed line calculated using "average" carbon Bragg curve - see text.

Fig. 6. $G^i(Fe^{3+})$ from aerated ferrous sulfate solutions irradiated with positive ions. Solid lines, C^{6+}, Ne^{10+}, Ar^{18+} (this work). Dashed lines, $^2H^+$, $^4He^{2+}$ (Ref. 4). Dotted lines, $^2H^+$, $^1H^+$ (Ref. 5). Δ, N^{7+} (Ref. 12). $\boxdot$, $^2H^+$, $^4He^{2+}$ (Ref. 13).

Fig. 7. $G^i_e + G^i_H$ as a function of Z^2/β^2. Solid line, this work. $\boxdot$, Ref. 18.

Fig. 8. $G^i(Fe^{3+})$ from aerated ferrous sulphate solutions irradiated with

heavy ions. Blocks are experimental, showing 1σ random error.

Solid lines are from model calculations (Ref. 10). Dotted lines

are fragmentation calculation (see text). For clarity, neon data

has been displaced down by two G value units and argon by four

units. Thus, $f(Z) = 0$ for carbon, 2 for neon and 4 for argon.
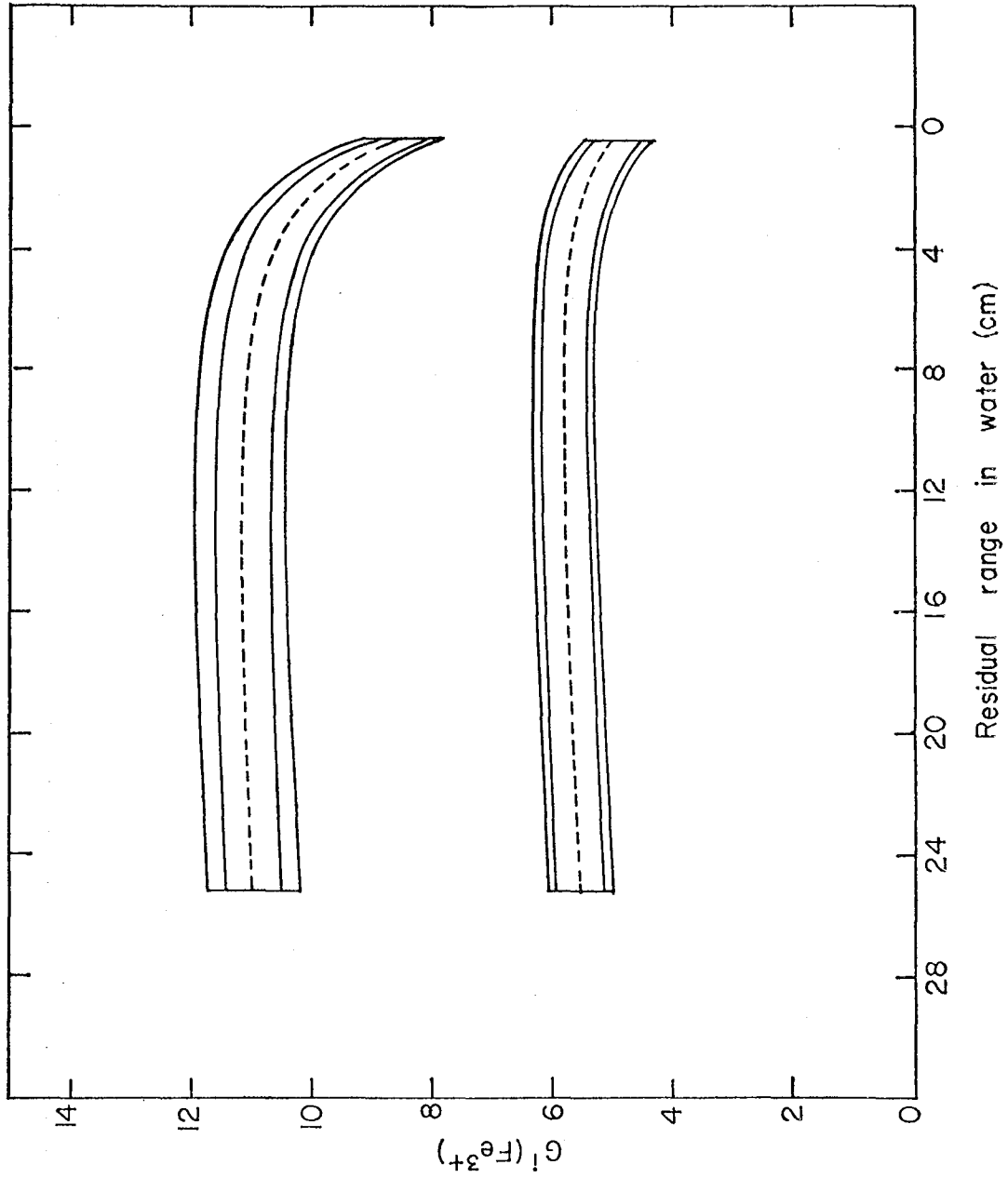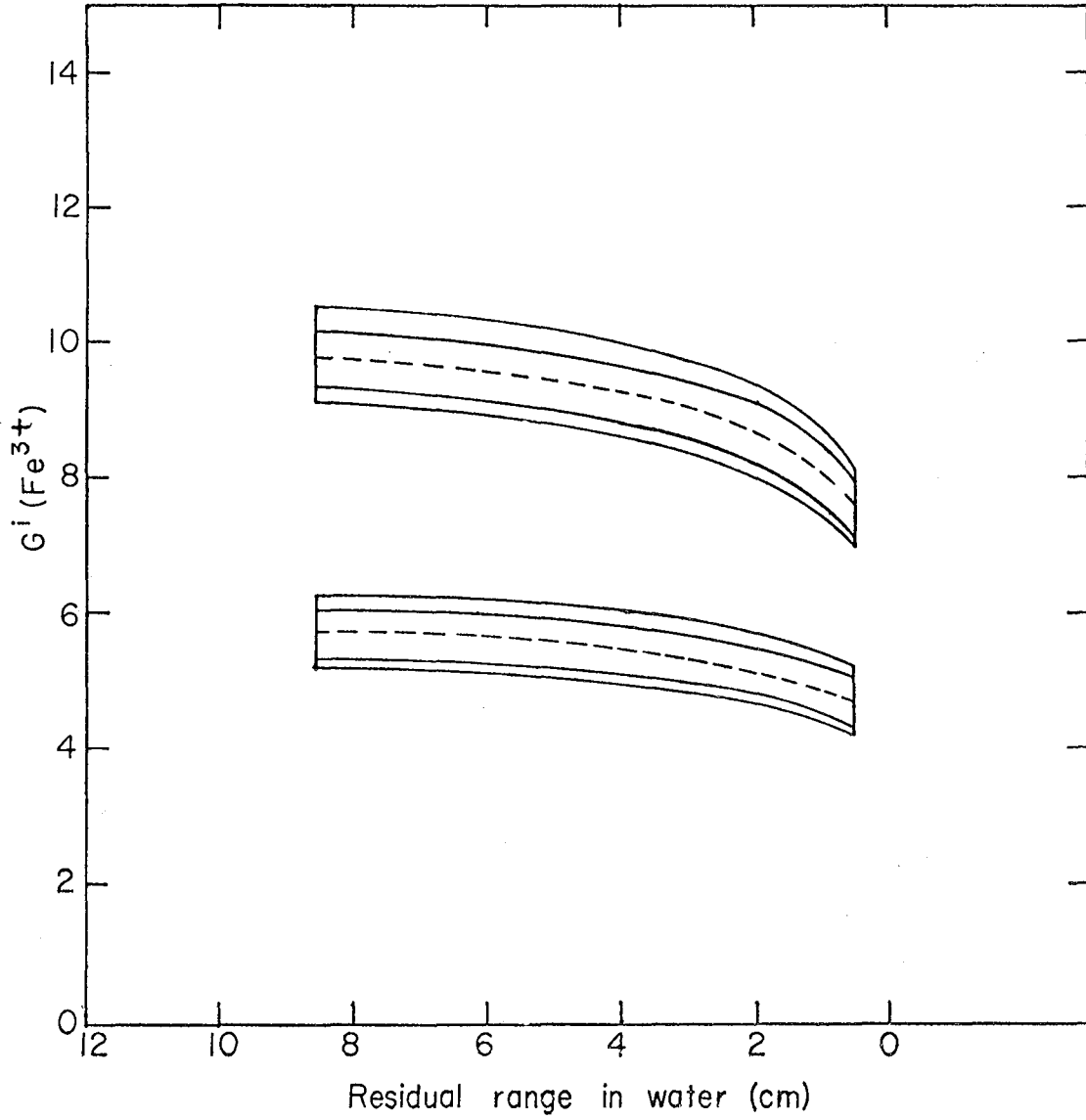
Fig. 1

XBL 807-10787

Fig. 2

XBL 807-10788

XBL 807-10789

Residual range in water (cm)

$G_i(Fe^{3+})$

Fig. 3

Fig. 4

XBL 807-10790

XBL 807-10791

Fig. 5

XBL 807-10792

Fig. 6

Fig. 7

XBL 807-10793

XBL 807-10794

Fig. 8